HHS Public Access

Author manuscript

Electrospinning. Author manuscript; available in PMC 2019 April 25.

Published in final edited form as:

Electrospinning. 2018 February ; 2(1): 15–28. doi:10.1515/esp-2018-0002.

Solvent retention in electrospun fibers affects scaffold mechanical properties

Anthony R. D'Amato[*],
Department of Biomedical Engineering, Rensselaer Polytechnic Institute, 110 8th St., Troy, New York 12180, United States of America; Center for Biotechnology and Interdisciplinary Sciences, Rensselaer Polytechnic Institute, 1623 15th Street, Troy, New York 12180, United States of America

Michael T. K. Bramson,
Department of Biomedical Engineering, Rensselaer Polytechnic Institute, 110 8th St., Troy, New York 12180, United States pf America

Devan L. Puhl,
Department of Biomedical Engineering, Rensselaer Polytechnic Institute, 110 8th St., Troy, New York 12180, United States of America; Center for Biotechnology and Interdisciplinary Sciences, Rensselaer Polytechnic Institute, 1623 15th Street, Troy, New York 12180, United States of America

Jed Johnson,
Nanofiber Solutions, 4389 Weaver Court North, Hilliard, OH 43026, United States of America

David T. Corr, and
Department of Biomedical Engineering, Rensselaer Polytechnic Institute, 110 8th St., Troy, New York 12180, United States pf America

Ryan J. Gilbert
Department of Biomedical Engineering, Rensselaer Polytechnic Institute, 110 8th St., Troy, New York 12180, United States of America; Center for Biotechnology and Interdisciplinary Sciences, Rensselaer Polytechnic Institute, 1623 15th Street, Troy, New York 12180, United States of America

Abstract

Electrospinning is a robust material fabrication method allowing for fine control of mechanical, chemical, and functional properties in scaffold manufacturing. Electrospun fiber scaffolds have gained prominence for their potential in a variety of applications such as tissue engineering and textile manufacturing, yet none have assessed the impact of solvent retention in fibers on the scaffold's mechanical properties. In this study, we hypothesized that retained electrospinning solvent acts as a plasticizer, and gradual solvent evaporation, by storing fibers in ambient air, will

[*]**Corresponding Author: Anthony R. D'Amato:** Department of Biomedical Engineering, Rensselaer Polytechnic Institute, 110 8th St., Troy, New York 12180, United States of America; Center for Biotechnology and Interdisciplinary Sciences, Rensselaer Polytechnic Institute, 1623 15th Street, Troy, New York 12180, United States of America.

cause significant increases in electrospun fiber scaffold brittleness and stiffness, and a significant decrease in scaffold toughness. Thermogravimetric analysis indicated solvent retention in PGA, PLCL, and PET fibers, and not in PU and PCL fibers. Differential scanning calorimetry revealed that polymers that were electrospun below their glass transition temperature (T_g) retained solvent and polymers electrospun above T_g did not. Young's moduli increased and yield strain decreased for solventretaining PGA, PLCL, and PET fiber scaffolds as solvent evaporated from the scaffolds over a period of 14 days. Toughness and failure strain decreased for PGA and PET scaffolds as solvent evaporated. No significant differences were observed in the mechanical properties of PU and PCL scaffolds that did not retain solvent. These observations highlight the need to consider solvent retention following electrospinning and its potential effects on scaffold mechanical properties.

Keywords

Electrospun fibers; Solvent retention; mechanical characterization

1 Introduction

Electrospinning is a robust material fabrication method that produces nano-to micro-scale non-woven meshes with a wide range of mechanical, chemical, and functional properties. Applications such as tissue engineering [1–5], drug delivery [6, 7], textile manufacturing [8], and filtration [9] frequently employ electrospun fiber scaffolds. In recent years, new, solvent-free electrospinning procedures have come to light. Solution electrospinning, which consists of first dissolving a polymer in a volatile organic solvent, however, remains the most common electrospinning method [10]. When a voltage is applied to the polymer solution, the solvent evaporates as fibers are deposited on the collection surface. It is important to consider solvent retention in fibers after fabrication, however, because many of the common solvents used in solution electrospinning are toxic.

A study by Nam *et al.* was one of the first studies to thoroughly explore solvent retention in electrospun fibers [11]. In that study, researchers electrospun PCL-gelatin blend fibers using 1,1,1,3,3,3-hexafluoroisopropanol (HFIP) as a solvent. The authors observed large amounts of residual HFIP in their fibers (as much as 16600 ppm) and determined that HFIP levels above 250 ppm adversely affected chondrocyte viability in culture. Our group, in a study by D'Amato *et al.*, explored retention of both HFIP and chloroform in poly(lactic acid) (PLA) fibers, and tested different approaches to facilitate solvent removal [12]. Surprisingly, fibers retained as much as 8.5% (weight of solvent with respect to weight of PLA) of chloroform or 15.5% of HFIP immediately after electrospinning. Retained solvent remained in fibers for as long as 28 days without employing post-fabrication techniques to facilitate solvent removal. A subsequent study revealed that HFIP retention influenced drug release kinetics from PLA fibers with the drug 6-aminonicatinomide (6AN) incorporated in the polymer matrix. Immediately after electrospinning, fibers with large amounts of residual HFIP released 6AN over 9 days, whereas fibers that were treated to remove solvent released 6AN for as long as 44 days [13]. With the effects of residual solvent already studied with regards

to cellular toxicity and drug delivery, another important aspect of electrospun fibers remains to be studied in the context of organic solvent retention fiber mechanical properties.

Most electrospun fiber applications occur in a dynamic environment (tissue engineering, filtration, textiles, etc.), where the fibrous scaffold is subjected to continuous or intermittent stress. From these examples, it is clear that fibers should possess specific mechanical properties to ensure proper function. In industry, plasticizers are often used to increase the amount of free-volume between polymer chains. This is common practice to increase the ductility of polymer products [14]. Residual solvent in electrospun fibers acts as a plasticizer and may affect electrospun fiber mechanical properties by increasing the free volume within individual fibers. This becomes a cause for concern since the aforementioned studies observed large amounts of solvent present in fibers immediately after electrospinning that decreased over time. This suggests that fibers, immediately after electrospinning, will have more free volume within the polymer matrix than they will at a later time point once solvent has evaporated. As a result, tensile testing shortly after electrospinning may misleadingly suggest that the fibers are far more flexible and ductile than they will be by the time they are applied.

The study herein explores this phenomenon in five different commonly-used electrospinning polymers, to determine if the mechanical properties of electrospun fiber mats change significantly over time as solvent leaves the fibers. We used thermogravimetric analysis (TGA) and differential scanning calorimetry (DSC) to quantify solvent retention in electrospun fibers and discern the mechanism by which various polymers may retain solvent differently. We then performed uniaxial tensile testing on each polymer fiber type over the course of fourteen days to determine if solvent retention significantly affected fiber elastic moduli, yield strain, failure strain, peak stress, and toughness. Our findings raise an important consideration in how and when fiber scaffolds should be mechanically characterized.

2 Experimental Procedures

2.1 Electrospun Fiber Fabrication

2.1.1 Electrospinning Apparatus—The electrospinning apparatus was completely enclosed within a 35 × 36 in. dissipative PVC glove box (Terra Universal, Fullerton, CA). Previous studies from the Gilbert laboratory show that fluctuations in the humidity of the electrospinning environment can drastically affect fiber diameter and surface topography [15, 16]. Thus, this enclosure was important to maintain the relative humidity of the electrospinning environment during fiber fabrication and prevent variations between fiber replicates. Within the glove box, a syringe pump was affixed above a grounded, spinning aluminum disk (22-cm diameter, 1-cm thick). A 5-mL syringe containing electrospinning solutions affixed to a 22 gauge needle (syringes and needles purchased through Becton-Dickenson, Franklin Lakes, NJ) was placed in the syringe pump and attached to a Gamma High Voltage Power Supply (Model No. ES5OP-10W, State College, PA). A collection distance of 5-cm was used between the needle tip and the collection wheel.

2.1.2 Electrospun Fiber Fabrication—In this study, we electrospun five different polymers that are commonly found in electrospinning literature, and that are all soluble in the solvent HFIP (Sigma-Aldrich, St. Louis, MO). We used this approach to directly compare solvent retention in the different polymers without differences in solvent, such as vapor pressure or boiling point, affecting the amount of solvent retained by each polymer. Poly(glycolic acid) (PGA, Purac), poly(L-lactide-co-caprolactone) (PLCL, Purac), poly(ethylene terephthalate) (PET, Auriga Polymers), and polycaprolactone (PCL, Sigma-Aldrich) solutions contained 10% (w/w) of polymer in HFIP. Polyurethane (PU, AdvanSource) solutions contained 5% (w/w) of polymer in HFIP due to the higher molecular weight leading to increased PU solution viscosity. All polymer solutions were electrospun with an applied voltage of 10 kV, rotational mandrel speed of 1000 rpm, solution flow rate of 2 mL/hr, and fiber collection time of 15 minutes. To obtain samples for scanning electron microscopy (SEM), fibers were collected on 15×15 mm glass coverslips (Knittel Glass, Brausenweig, Germany) during electrospinning. Fibers for TGA were deposited directly onto the rotating mandrel and carefully lifted off of the wheel immediately after electrospinning. Fibers were then analyzed or stored in ambient lab conditions (atmospheric pressure, and room temperature ranging from 21–25◦C) until the appropriate time point for testing.

For mechanical characterization, fibers were electrospun directly into oaktag I-frames specimen holders (used for tensile testing) taped to the 1-cm wide rotating mandrel (Figure 1A), to allow for consistent, and relatively easy, fabrication of material tensile test specimens. Custom I-frames with a 30-mm intra-arm spacing were utilized to create specimens with a target aspect ratio of 3.0 (*i.e.* 30-mm gauge length, and 10-mm width). After electrospinning, samples were cut on the outside of the I-frame with a razor blade and sandwiched within the I-frame with a double-sided piece of tape that held the fibers in place (Figure 1B). Directly electrospinning into the I-frame specimen holders greatly reduced the amount of sample handling required to create a tensile specimen. This minimized specimen damage associated with mounting and gripping fibers prior to mechanical characterization (Figure 1C).

2.1.3 Scanning Electron Microscopy—Electrospun fiber scaffolds were imaged via SEM to measure specimen thickness and ensure that fiber morphology was consistent among independently electrospun samples of each polymer. This was necessary since differences in fiber diameter, collection density, or alignment may confound TGA and mechanical testing results. Prior to SEM, all scaffolds were first coated with a 1-nm thick layer of gold-palladium using a Technics Hummer V sputter coater (Anatech Ltd., Denver, CO). Fibers were then imaged using a FEI Versa 3D DualBeam SEM (Hillsboro, OR) with a low accelerating voltage (2–4 kV) to avoid melting fibers while imaging.

2.1.4 Morphological Characterization of Electrospun Fibers—SEM images of fibers were analyzed using FIJI software to characterize fiber physical properties including diameter, collection density, and alignment. Fiber diameter was characterized by drawing a line spanning the width of an individual fiber and converting the pixel length of the line to microns using the scale bar in each SEM image. This was done for 50 fibers from each

electrospinning replicate for a total of 150 diameter measurements for each polymer type. Fiber collection density was quantified by counting the number of fibers in a given SEM image and dividing by the width of the field of view to yield a value with units of fibers/mm. This value was then multiplied by fiber diameter, for each scaffold replicate, to yield a value for fiber coverage. Fiber coverage is represented as a percentage where 100% would indicate complete fiber coverage with no void space in between fibers. Finally, fiber alignment was characterized by drawing a line parallel to fiber orientation for all fibers in a given SEM image. The mean angle of all lines was then calculated, and the deviation of each fiber's angle from the mean was binned to determine the amount of fibers with a certain degree of deviation from the mean fiber alignment. Because fiber alignment has a strong potential to significantly affect fiber mechanical characterization, we used the Fast Fourier Transform (FFT) of fiber SEM images as a secondary method to measure fiber alignment [17]. A description of our FFT analysis, and results can be found in the supplemental information document that accompanies this manuscript. Alignment was measured in three separate SEM images taken from three separate fiber replicates for each polymer.

2.2 Thermogravimetric Analysis

Thermogravimetric analysis (TGA) was used to analyze the amount of solvent retained within fibers after electrospinning. TGA records specimen weight as temperature increases. Any weight reductions occurring between 50◦C and 90◦C were attributed to solvent evaporation, as was done in a previous study that validated this method for analyzing HFIP retention in electrospun fibers [12]. In that study, we used FTIR and NMR to ensure that weight reductions observed during TGA were attributable to solvent losses and not water from ambient humidity that may have adsorbed to fibers during experimentation. A Q50 Thermogravimetric Analyzer (TA Instruments, New Castle, DE) was used to conduct TGA. Fiber samples weighing approximately 15 mg were placed in a ceramic TGA crucible (TA Instruments) and exposed to a 15◦C/min heating ramp up to 400◦C. All polymer fibers were analyzed via TGA immediately after electrospinning (day 0). In cases where TGA at day 0 indicated solvent retention, additional fibers from the same electrospinning batch were also analyzed via TGA 1, 7, and 14 days after fabrication to analyze changes in the amount of retained solvent over time. Three independently prepared polymer solutions were electrospun to create three distinct sets of fibers for TGA (N=3), and weight% change values are reported as the mean ± standard deviation.

2.3 Differential Scanning Calorimetry

After observing differences in solvent retention among the various polymers, differential scanning calorimetry (DSC) was used to analyze the glass transition temperatures (T_g) of each raw polymer, before any processing. This was done to discern whether each polymer was electrospun above or below its respective T_g. We hypothesized that polymers electrospun above T_g would not retain solvent and polymers electrospun below T_g would retain solvent. This hypothesis was supported by the fact that polymer chains within electrospun fibers have higher mobility above T_g, which would allow for easier solvent evaporation during fiber fabrication, and higher solvent retention in polymers below T_g with less mobile polymer chains. To perform DSC, 5 mg of raw polymer (prior to electrospinning) was placed into a hermetic DSC pan (TA Instruments) and a hermetic DSC

lid (TA Instruments) was crimped onto the pan. DSC was then performed by heating samples from −20◦C to 400◦C at a rate of 10◦C/min using a TA Instruments DSC-Q100. DSC curves were analyzed using TA Universal Analysis software. The midpoint of the glass transition region in each DSC curve was recorded as the T_g for each polymer sample. Each polymer was analyzed via DSC in triplicate (N=3), where three separate polymer samples were analyzed. All T_g values are reported as the mean ± standard deviation.

2.4 Mechanical Characterization

After measuring specimen width using a digital caliper, test specimens were secured in a vertical Universal Testing machine (Model 500LE2–1, TestResources, Shakopee, MN), equipped with a 500 g load cell. Each specimen was secured in the upper grip, lowered, and then secured in the lower grip. Once gripped, the supporting I-frame was transected, leaving only the material test specimen spanning grip-to-grip (Figure 1C). Specimen gauge length was measured using a digital caliper, and load was zeroed. To mechanically characterize, the specimen was elongated to failure at a constant rate (0.5 mm/s), while force, grip-to-grip displacement, and time data were acquired at 50 Hz. All mechanical characterization was performed in triplicate (N=3) using three independently fabricated electrospun fiber samples for each polymer, at each of the four time points used in solvent retention analysis: immediately after electrospinning (day 0), and 1, 7, and 14 days after fabrication. This experimental design allowed us to determine if the mechanical properties of fibers changed significantly as residual solvent was leaving the fibers over time.

2.5 Data Analysis and Statistics

Raw force-displacement data were filtered using a 6.5 Hz lowpass filter to remove periodic noise. Filtered force and displacement data were normalized by original specimen cross-sectional area and gauge length, respectively, to convert to values of engineering stress and engineering strain. The resulting stress-strain curves were analyzed to compute yield strain, Young's elastic moduli, peak stress, failure strain, and failure toughness (energy to the point of initial failure). All of the polymers, except for PU, exhibited a bimodal response to tensile loading, with a clear point of yield. To calculate elastic moduli from the stress-strain curves, the slope was determined from a linear fit over the red shaded region (Figure 2), and the yield strain was defined as the intersection of the two lines fit to the red and green shaded regions in Figure 2, denoted with a black arrow. Failure toughness was calculated as the area under the stress-strain curve, from the onset of strain to the point of failure (denoted as a red asterisk in Figure 2), using trapezoidal integration.

Fiber morphological data, as well as TGA, DSC, and mechanical properties are reported as means ± standard deviations. Statistical analyses were conducted using a one-way analysis of variance (ANOVA) followed by Post Hoc Student's t-test, with $p<0.05$ considered statistically significant.

3 Results

3.1 Electrospun Fiber Fabrication and SEM

Figure 3 shows SEM images of fibers that were electrospun using each of the five aforementioned polymers. These images were analyzed using FIJI software to characterize fiber diameter, collection density, and alignment and results are displayed in Table 1. Fiber diameters were consistent among independently fabricated replicates for each polymer type, but varied largely between certain polymers. This held true for fiber collection density and fiber coverage. Lastly, fiber alignment was extremely consistent among all polymer types, and between replicates of each fiber type, as all polymer fibers were highly aligned.

3.2 Solvent Retention Analysis

TGA revealed that three of the five polymers, PGA, PLCL, and PET, exhibited significant reductions in sample weight immediately after electrospinning, which indicated solvent retention (Figure 4A). At this initial time point, PGA underwent a 7.8±0.7% weight reduction. This weight reduction in PGA fibers decreased to 5.4±0.2 after 1 day, 4.4±0.5 after 7 days, and 3.9±0.3% 14 days after electrospinning. PLCL fibers showed a 5.4±1.8% reduction in sample weight immediately after electrospinning. This value decreased to 1.6±0.8, 0.3±0.2, and 0.1±0.0% on days 1, 7, and 14 respectively. PET fibers exhibited a larger reduction in weight% than other polymers that were analyzed. Immediately after electrospinning, PET fibers showed a 16.9±0.2% reduction in sample weight. This value decreased to 11.8±0.7, 9.3±0.3, and 8.3±0.4% on days 1, 7, and 14 respectively. We attributed all weight reductions to retained solvent evaporating out of the fibers, as was validated via NMR and FTIR in a previous study conducted in our lab [12].

In contrast to the three aforementioned polymers, TGA revealed weight reductions of 0.1±0.1 and 0.2±0.1% in PU and PCL, respectively, immediately after electrospinning. These values, and the variations between replicates, were attributed to fluctuations in the TGA instrumentation, as the instrument's precision is ±0.1%. We concluded, therefore, that PU and PCL did not retain HFIP after electrospinning.

3.3 Glass Transition Temperature Analysis

TGA revealed that only PGA, PLCL, and PET electrospun fibers retained significant amounts of HFIP while PU and PCL electrospun fibers did not. We hypothesized that polymers with T_g values below room temperature would not retain solvent after electrospinning due to the amorphous nature of the polymer, *e.g.* higher polymer chain mobility, allowing for easier, rapid solvent evaporation during electrospinning. In contrast, we hypothesized that glassy polymers, with T_g values above room temperature, would retain solvent due to the decreased rate of solvent diffusion out of fibers during electrospinning resulting from decreased polymer chain mobility. T_g values for PGA, PLCL, and PET, were 39.4±2.2, 48.1±0.6, and 74.3±0.9◦C, respectively (Figure 4B). All three of these polymers retained solvent after electrospinning. T_g values for PU and PCL were −14.8±2.9 and −5.9±2.8◦C, respectively, and these polymers did not retain solvent after electrospinning. The ambient temperature in the Gilbert lab electrospinning environment fluctuated between 21◦C and 22◦C during all electrospinning runs, as depicted by the dashed line in Figure 4B.

This fact, combined with T_g values for all polymers used in this study, allowed us to validate our hypothesis that polymer T_g would affect a polymer's ability to retain solvent during electrospinning.

3.4 Fiber Scaffold Mechanical Testing

By directly electrospinning into I-frames, we were able to produce tensile test specimens with consistent geometries, and aspect ratios ≥ 3.0, for each polymer (Table S2). This allowed us to mechanically characterize specimens of all five polymer fiber types, at each of the four time points corresponding to our solvent-retention analyses, to explore whether the fiber mechanical properties changed over the 14-day period. We hypothesized that solvent-retaining polymers would become stiffer, more brittle, and less tough as solvent left the fibers, while polymers that did not retain solvent would show no difference in mechanical properties over time. All mechanical testing data are summarized and included in Table S2 in the supplemental information.

3.4.1 Elastic Modulus—Figure 5 displays elastic moduli for each polymer fiber type. The moduli of all three polymers that retained solvent (PGA, PLCL, and PET) increased over time. This validated our hypothesis that solvent-retaining polymer fibers would become stiffer as solvent left the fibers. The modulus of PGA fibers was 1013.4±209.6 MPa immediately after electrospinning. This value increased nearly three-fold to 2989.1±492.5 MPa 14 days after electrospinning. PLCL fibers, although far more elastic than PGA fibers, exhibited similar stiffening behavior. Immediately after electrospinning, the modulus of PLCL fibers was 42.4±4.9 MPa. After 14 days of solvent leaving the fibers, this value increased greater than four-fold to a value of 188.9±127.6 MPa. Following suit with PGA and PLCL, the modulus of PET fibers increased significantly over 14 days from 589.1±362.7 MPa to 1518.6±359.2 MPa. PU and PCL, the two polymers that did not retain solvent after electrospinning, exhibited no statistically significant changes in modulus over the first fourteen days following fiber fabrication.

3.4.2 Yield Strain and Failure Strain—Figure 6A displays yield strain values recorded for each polymer type during tensile testing. The three polymers that retained solvent in this study, PGA, PLCL, and PET, yielded at significantly lower strains at all time points later than the initial test conducted immediately after electrospinning. At the initial time point, PGA, PLCL, and PET yielded at 3.5±1.4%, 4.0±0.4%, and 4.1±1.2% strain, respectively. After one day, yield strain decreased significantly and reached final values of 1.5±0.1%, 2.3±0.0%, and 3.1±0.6% for PGA, PLCL, and PET, respectively. Interestingly, PCL, which did not retain solvent, yielded at a significantly higher strain one day after electrospinning. PCL yielded at 4.3±1.0% strain immediately after electrospinning, and yielded at 7.0±1.0% strain one day after electrospinning. PCL yield strain values at all other time points, however, were not statistically significant when compared to values immediately after electrospinning. Yield strain data for PU is not presented in Figure 6A because PU did not exhibit yielding behavior prior to failure.

Failure strain (Figure 6B) exhibited trends similar to those seen in Figure 6A for PGA, PLCL, and PET. The differences observed in failure strain, however, were not statistically

significant in PLCL. PGA and PET fibers failed at significantly lower strain values at all time points past day 0. Immediately after electrospinning, PGA and PET fibers failed at 20.0±3.3% and 231.0±32.1% strain, respectively. Fourteen days after electrospinning, these values decreased significantly to 8.9±2.6% and 19.7±2.6% strain for PGA and PET, respectively. These changes represent an approximate two-fold decrease in failure strain for PGA, and an eleven-fold decrease in PET fiber failure strain. Unexpectedly, the failure strain of PU fibers at day 7 (142.1±2.9%) was significantly higher than the failure strain observed immediately after electrospinning (126.6±8.0%).

3.4.3 Peak Stress and Toughness—Figure 7A shows peak stress values for all polymer fiber types immediately after electrospinning and 1, 7, and 14 days after fiber fabrication. PLCL was the only polymer where peak stress changed significantly after the initial testing time point. Immediately after electrospinning, the peak stress of PLCL fibers was 36.2±6.9 MPa. This value increased significantly to a final value of 56.0±12.4 MPa 14 days after electrospinning.

Failure toughness was calculated for each polymer at each time point by integrating stress-strain curves to the point of failure (Figure 7B). PGA fibers became significantly less tough over 14 days, decreasing from an initial toughness of 6.8±2.3 J/m3 to a final value of 3.6±1.1 J/m3 after 14 days. PET fibers also became significantly less tough as solvent left the fibers over time. Immediately after electrospinning, the toughness of PET fibers was 57.8±14.4 J/m3, and this value decreased to 6.5±0.5 J/m3 after 14 days. Failure toughness did not change significantly in any of the other polymers over the course of experimentation.

4 Discussion

The major findings of this study were: 1) Solvent retention varies between different polymers after electrospinning, and this may be the result of differences in T_g among polymers, 2) The mechanical properties of fibers that retain solvent after electrospinning can change significantly over time as solvent leaves the fibers. Both of these findings are important when considering electrospun fibers for any application; particularly applications where differences in fiber mechanical properties can impact outcomes, such as tissue engineering, or lead to scaffold failure, such as in textile manufacturing or filtration. The data presented here can help inform whether any post-fabrication drying methods are necessary to ensure consistency in material characterization and performance.

Prior to any thermal or mechanical testing, we assessed consistency in fiber morphology between fiber replicates of the same polymer. Morphological consistency is vital since the physical characteristics of fibers, such as diameter and alignment, can influence mechanical characteristics [18–20]. A study by Stylianopoulos and colleagues showed that changes in fiber diameter and alignment can influence fiber modulus measurements by nearly six-fold [19]. Further, Mubyana and colleagues showed that changing fiber alignment and scaffold thickness led to significant changes in fiber scaffold modulus, peak stress, failure strain, and toughness [18]. SEM of fiber samples (Figure 3) and subsequent morphological analysis (Table 1) confirmed consistency between fiber physical characteristics within each polymer

type between the different electrospinning batches. As such, we confirmed that physical properties of fibers did not vary between individual electrospinning batches.

Once we electrospun fibers from each polymer reproducibly, TGA revealed significant amounts of solvent were retained in PGA, PLCL, and PET fibers, while PU and PCL fibers did not retain solvent. Additional experiments were not conducted here to confirm that weight reductions in TGA were entirely due to the removal of retained solvent. However, a previous study by our group validated that TGA weight reductions occurred from solvent removal by using FTIR and NMR as chemically-specific analytical methods [12]. That study proved that weight reductions were not attributable to losses of water that may have adsorbed to fiber scaffolds over the course of experimentation. Thus, in this study, FTIR and NMR were not used, and TGA was used solely to measure solvent retention over time.

We hypothesized that the observed difference in solvent retention between different polymers was a consequence of differences in each polymer's respective T_g value. We validated this hypothesis by using DSC to analyze T_g values of each of the five polymers. Polymers electrospun below their T_g retained solvent, and polymers electrospun above their T_g did not. Fibers that are electrospun at environmental temperatures above their T_g contain polymer chains with higher mobility, which allows for easier evaporation of solvent during fiber formation. In contrast, polymers electrospun at environmental temperatures below their T_g are glassy, and solvent evaporation out of fibers is slowed due to the decrease in polymer chain mobility, thus explaining why these fibers retained solvent. These findings are supported by a study from Tihminlioglu *et al.*, where solvent removal from a 3-μm thick polystyrene coating is slowed when the polymer is formed below its T_g [21]. Although the Tihminlioglu *et al.* study did not analyze electrospun fibers, their findings support our observations.

After observing significant amounts of solvent retained within three types of polymer fibers (PGA, PLCL, and PET), we hypothesized that retained solvent would influence fiber scaffold mechanical properties as solvent evaporated out of the fibers over time. Our hypothesis is based on the extensive use of plasticizers in polymer systems. Frequently, plasticizers are incorporated into many industrial plastics to improve ductility [14]. Thus, one could think of retained solvent in fibers as a plasticizer, and fibers would exhibit increased ductility initially. As solvent is removed, the fibers become less ductile and more rigid. This correlation is supported by a study incorporating different amounts of plasticizers into poly-lactic acid (PLA) films [22]. Baiardo and colleagues used as little as 5% (w/w) of the plasticizers poly(ethylene glycol) or acetyl tri-n-butyl citrate in their films, and observed significant changes in film modulus, tensile strength, and failure strain. In our study, we observed as little as 5.4% of retained solvent in PLCL fibers, and as much as 16.9% of retained solvent in PET fibers immediately after electrospinning. Our results are in agreement with the findings by Baiardo and colleagues. At day 0 (immediately after electrospinning) the amount of HFIP in PGA, PLCL, and PET is highest. For all three of these polymers, flexibility was highest (lowest elastic modulus) at day 0, as were yield strain and strain at failure (PLCL failure strain was not statistically different). Each of these polymers exhibited an increase in elastic modulus over time, which was accompanied by a significant decrease in failure strain. However, these polymers did not get stronger, as there

was no appreciable change in peak stress over time. Together, these findings indicate that the fibers stiffen and become much more brittle as they lose solvent, which is reflected in concomitant reductions in toughness. This effect was most pronounced in those polymers that retained the greatest amount of solvent, *e.g.*, PET, suggesting that the retained solvent was providing viscoelasticity to the polymer, making it more compliant and granting it greater extensibility. Thus, we validated the hypothesis that retained solvent would influence fiber properties, such that the polymers would become stiffer and more brittle as the retained solvent evaporated with time. Future viscoelastic studies, exploring strain-rate sensitivity, creep and/or stress relaxation behaviors, as well as how these change with the loss of solvent over time, could provide further insight into the source of this stiffening and embrittlement with the loss of retained solvent. These further tests may also help elucidate why polymers that did not retain solvent (PU and PCL) exhibited some changes in mechanical properties over time (a spike in PCL yield strain on day 1, and a slight increase in PU failure strain on day 7), although these changes were far less frequent than in solvent-retaining polymer fibers.

The most significant solvent-mediated changes in fiber mechanical properties were observed in elastic modulus measurements. Comparing mechanical property data from day 0 and day 14 fibers, the elastic moduli of PGA, PLCL, and PET fibers increased by at least a factor of 2.5 (for PET fibers) and as much as a factor of 4.5 (for PLCL fibers). This increase in modulus over time is an important consideration for many different applications, especially tissue engineering. Multiple studies show the ability of material stiffness to influence stem cell differentiation [23]. Engler *et al.* cultured naïve mesenchymal stem cells (MSCs) on different polyacrylamide gels of varying stiffness ranging from 0.1 to 40 kPa, and specific gels induced unique cell differentiation [24]. The softer gel similar to the modulus of brain tissue led MSCs to a neurogenic fate. In contrast, a stiffer gel, similar in stiffness to bone, led MSCs to an osteogenic fate. A gel with a modulus in between these two, comparable to skeletal muscle stiffness, induced differentiation towards a myogenic fate. The difference in the moduli between these gels were as low as two-fold (between myogenic and osteogenic fate inducing gels), which is within the variation in modulus that we observed in this study. Importantly, the difference between moduli in the Engler *et al.* study and the data we present is approximately three orders of magnitude. This suggests that although the observations in the current study may affect tissue engineering outcomes, stem cell differentiation may not be affected. Kim and colleagues, however, fabricated composite polymer scaffolds for bone tissue engineering with initial compressive and tensile moduli of 2.3 and 2.0 MPa, respectively. The researchers then created scaffolds with compressive and tensile moduli that were increased by two and thirteen-fold, respectively. Osteoblasts cultured on scaffolds with increased moduli significantly increased cell proliferation, alkaline phosphatase activity, and calcium deposition compared to osteoblasts cultured on scaffolds with lower moduli [25]. As the fibrous polymer scaffolds studied here have similar moduli in the MPa range, this suggests that the changes that we observed could impact bone tissue engineering outcomes. The importance of changes in fiber mechanical properties in tissue engineering applications, however, may be overshadowed by the toxicity of HFIP retained within fibers. HFIP is toxic to cells in the low millimolar range [26]. Thus, depending on how quickly HFIP diffuses out of fibers, the toxicity effects may have a larger impact on tissue engineering outcomes than

the effects of changing mechanical properties. To prevent either of these unwanted circumstances, all electrospinning scaffolds should be completely dried of solvent prior to any characterization or implementation in tissue engineering applications.

While material modulus is important for tissue engineering applications, the other mechanical properties examined here (such as material yield strain and strain at failure) are likely more important for other, non-biological applications of electrospun fibers. Immediately after electrospinning, PGA, PLCL, and PET fibers yielded at a significantly higher strain than what was observed at all later time points. Further, at all time points after day 0, PGA and PET fiber mats failed at strain values that were reduced by two-fold and eleven-fold, respectively. These findings are important for applications such as filtration where fibers may be under constant strain due to liquid or air flow through the mesh. A study by Huang and colleagues emphasizes the necessity to enhance the tensile strength of electrospun membranes for filtration purposes as this property is commonly the downfall of fiber membranes used for filtration [27]. Further, Kaur *et al.* demonstrated that increasing the yield stress, tensile strength, and strain at break for electrospun filtration membranes led to increased filtration performance at higher pressures [28]. Thus, if fiber scaffolds are not properly characterized prior to this application they may fail unexpectedly. In total, we provide data to encourage all electrospinning practitioners to consider solvent retention effects on the mechanical properties of their fibrous materials.

5 Conclusions

The findings here stipulate the need for solvent removal from electrospun fibers prior to mechanical characterization as retained solvent can significantly affect mechanical properties. Polymer T_g was an effective predictor of solvent retention for all polymers tested in this study. Polymers electrospun below T_g retained solvent, and polymers electrospun above T_g did not. Further, solvent retention resulted in as much as an eleven-fold change in mechanical properties over the course of fourteen days. Thus, this study should draw attention to the consistency and rigor that is required to ensure that fibers are produced, dried, and tested carefully to maintain reproducibility.

Supplementary Material

Refer to Web version on PubMed Central for supplementary material.

Acknowledgement:

This work was funded by NSF CAREER Award grant (1105125) and NIH R01 grant (NS092754) to RJG. We also wish to acknowledge the funding support provided by The New York State Spinal Cord Injury Research Board (NYSSCIRB) Predoctoral Fellowship Award (Contract# C32631GG) awarded to ARD.

References

[1]. Zhang C, Wang X, Zhang E, Yang L, Yuan H, Tu W, Zhang H, Yin Z, Shen W, Chen X, Zhang Y, Ouyang H, An epigenetic bioactive composite scaffold with well-aligned nanofibers for functional tendon tissue engineering, Acta Biomater 66 (2018) 141–156. doi:10.1016/j.actbio.2017.09.036. [PubMed: 28963019]

[2]. Baek J, Sovani S, Choi W, Jin S, Grogan SP, D'Lima DD, Meniscal Tissue Engineering Using Aligned Collagen Fibrous Scaffolds: Comparison of Different Human Cell Sources, Tissue Eng. Part A 24 (2017) 81–93. doi:10.1089/ten.tea.2016.0205. [PubMed: 28463545]

[3]. Jiang L, Wang L, Wang N, Gong S, Wang L, Li Q, Shen C, Turng L-S, Fabrication of polycaprolactone electrospun fibers with different hierarchical structures mimicking collagen fibrils for tissue engineering scaffolds, Appl. Surf. Sci 427 (2018) 311–325. doi:10.1016/j.apsusc.2017.08.005.

[4]. Young BM, Shankar K, Allen BP, Pouliot RA, Schneck MB, Mikhaiel NS, Heise RL, Electrospun Decellularized Lung Matrix Scaffold for Airway Smooth Muscle Culture, ACS Biomater. Sci. Eng 3 (2017) 3480–3492. doi:10.1021/acsbiomaterials.7b00384.

[5]. Puperi DS, Kishan A, Punske ZE, Wu Y, Cosgriff-Hernandez E, West JL, Grande-Allen KJ, Electrospun Polyurethane and Hydrogel Composite Scaffolds as Biomechanical Mimics for Aortic Valve Tissue Engineering, ACS Biomater. Sci. Eng 2 (2016) 1546–1558. doi:10.1021/acsbiomaterials.6b00309.

[6]. Hu X, Liu S, Zhou G, Huang Y, Xie Z, Jing X, Electrospinning of polymeric nanofibers for drug delivery applications, J. Controlled Release 185 (2014) 12–21. doi:10.1016/j.jconrel.2014.04.018.

[7]. Liu S, Pan G, Liu G, das Neves J, Song S, Chen S, Cheng B, Sun Z, Sarmento B, Cui W, Fan C, Electrospun fibrous membranes featuring sustained release of ibuprofen reduce adhesion and improve neurological function following lumbar laminectomy, J. Controlled Release 264 (2017) 1–13. doi:10.1016/j.jconrel.2017.08.011.

[8]. Hsu Y-H, Chan C-H, Tang WC, Alignment of Multiple Electrospun Piezoelectric Fiber Bundles Across Serrated Gaps at an Incline: A Method to Generate Textile Strain Sensors, Sci. Rep 7 (2017). doi:10.1038/s41598-017-15698-7.

[9]. Peter KT, Johns AJ, Myung NV, Cwiertny DM, Functionalized polymer-iron oxide hybrid nanofibers: Electrospun filtration devices for metal oxyanion removal, Water Res 117 (2017) 207–217. doi:10.1016/j.watres.2017.04.007. [PubMed: 28399482]

[10]. Zhang B, Yan X, He H-W, Yu M, Ning X, Long Y-Z, Solventfree electrospinning: opportunities and challenges, Polym. Chem 8 (2017) 333–352. doi:10.1039/C6PY01898J.

[11]. Nam J, Huang Y, Agarwal S, Lannutti J, Materials selection and residual solvent retention in biodegradable electrospun fibers, J. Appl. Polym. Sci 107 (2008) 1547–1554. doi:10.1002/app.27063.

[12]. D'Amato AR, Schaub NJ, Cardenas JM, Franz E, Rende D, Ziemba AM, Gilbert RJ, Evaluation of procedures to quantify solvent retention in electrospun fibers and facilitate solvent removal, Fibers Polym 18 (2017) 483–492. doi:10.1007/s12221-017-1061-5.

[13]. D'Amato AR, Schaub NJ, Cardenas JM, Fiumara AS, Troiano PM, Fischetti A, Gilbert RJ, Removal of retained electrospinning solvent prolongs drug release from electrospun PLLA fibers, Polymer 123 (2017) 121–127. doi:10.1016/j.polymer.2017.07.008. [PubMed: 29200507]

[14]. Rahman M, Brazel CS, The plasticizer market: an assessment of traditional plasticizers and research trends to meet new challenges, Prog. Polym. Sci 29 (2004) 1223–1248. doi:10.1016/j.progpolymsci.2004.10.001.

[15]. Schaub NJ, D'Amato AR, Mason A, Corr DT, Harmon EY, Lennartz MR, Gilbert RJ, The effect of engineered nanotopography of electrospun microfibers on fiber rigidity and macrophage cytokine production, J. Biomater. Sci. Polym. Ed 28 (2017) 1303–1323. doi:10.1080/09205063.2017.1321345. [PubMed: 28420296]

[16]. Schaub NJ, Britton T, Rajachar R, Gilbert RJ, Engineered Nanotopography on Electrospun PLLA Microfibers Modifies RAW 264.7 Cell Response, ACS Appl. Mater. Interfaces 5 (2013) 10173–10184. doi:10.1021/am402827g. [PubMed: 24063250]

[17]. Ayres CE, Shekhar Jha B, Meredith H, Bowman JR, Bowlin GL, Henderson SC, Simpson DG, Measuring fiber alignment in electrospun scaffolds: a user's guide to the 2D fast Fourier transform approach, J. Biomater. Sci. Polym. Ed 19 (2008) 603–621. doi:10.1163/156856208784089643. [PubMed: 18419940]

[18]. Mubyana K, Koppes RA, Lee KL, Cooper JA, Corr DT, The influence of specimen thickness and alignment on the material and failure properties of electrospun polycaprolactone nanofiber mats,

J. Biomed. Mater. Res. A 104 (2016) 2794–2800. doi:10.1002/jbm.a.35821. [PubMed: 27355844]

[19]. Stylianopoulos T, Bashur CA, Goldstein AS, Guelcher SA, Barocas VH, Computational predictions of the tensile properties of electrospun fibre meshes: Effect of fibre diameter and fibre orientation, J. Mech. Behav. Biomed. Mater 1 (2008) 326–335. doi:10.1016/j.jmbbm.2008.01.003. [PubMed: 19627797]

[20]. McClure MJ, Sell SA, Ayres CE, Simpson DG, Bowlin GL, Electrospinning-aligned and random polydioxanonepolycaprolactone–silk fibroin-blended scaffolds: geometry for a vascular matrix, Biomed. Mater 4 (2009) 055010. doi:10.1088/1748-6041⁄4/5/055010. [PubMed: 19815970]

[21]. Tihminlioglu F, Danner RP, Solvent diffusion in amorphous polymers: Polystyrene–solvent systems, J. Polym. Sci. Part B Polym. Phys 38 (2000) 1965–1974. doi:10.1002/1099-0488(20000801)38:15<1965::AID-POLB20>3.0.CO;2-P.

[22]. Baiardo M, Frisoni G, Scandola M, Rimelen M, Lips D, Rufleux K, Wintermantel E, Thermal and mechanical properties of plasticized poly(L-lactic acid), J. Appl. Polym. Sci 90 (2003) 1731–1738. doi:10.1002/app.12549.

[23]. Lutolf MP, Gilbert PM, Blau HM, Designing materials to direct stem-cell fate, Nature 462 (2009) 433–441. doi:10.1038/nature08602. [PubMed: 19940913]

[24]. Engler AJ, Sen S, Sweeney HL, Discher DE, Matrix Elasticity Directs Stem Cell Lineage Specification, Cell 126 (2006) 677–689. doi:10.1016/j.cell.2006.06.044. [PubMed: 16923388]

[25]. Kim S-S, Sun Park M, Jeon O, Yong Choi C, Kim B-S, Poly(lactide-co-glycolide)/hydroxyapatite composite scaffolds for bone tissue engineering, Biomaterials 27 (2006) 1399–1409. doi:10.1016/j.biomaterials.2005.08.016. [PubMed: 16169074]

[26]. Capone R, Quiroz FG, Prangkio P, Saluja I, Sauer AM, Bautista MR, Turner RS, Yang J, Mayer M, Amyloid-β-Induced Ion Flux in Artificial Lipid Bilayers and Neuronal Cells: Resolving a Controversy, Neurotox. Res 16 (2009) 1–13. doi:10.1007/s12640-009-9033-1. [PubMed: 19526294]

[27]. Huang L, Manickam SS, McCutcheon JR, Increasing strength of electrospun nanofiber membranes for water filtration using solvent vapor, J. Membr. Sci 436 (2013) 213–220. doi:10.1016/j.memsci.2012.12.037.

[28]. Kaur S, Barhate R, Sundarrajan S, Matsuura T, Ramakrishna S, Hot pressing of electrospun membrane composite and its influence on separation performance on thin film composite nanofiltration membrane, Desalination 279 (2011) 201–209. doi:10.1016/j.desal.2011.06.009.

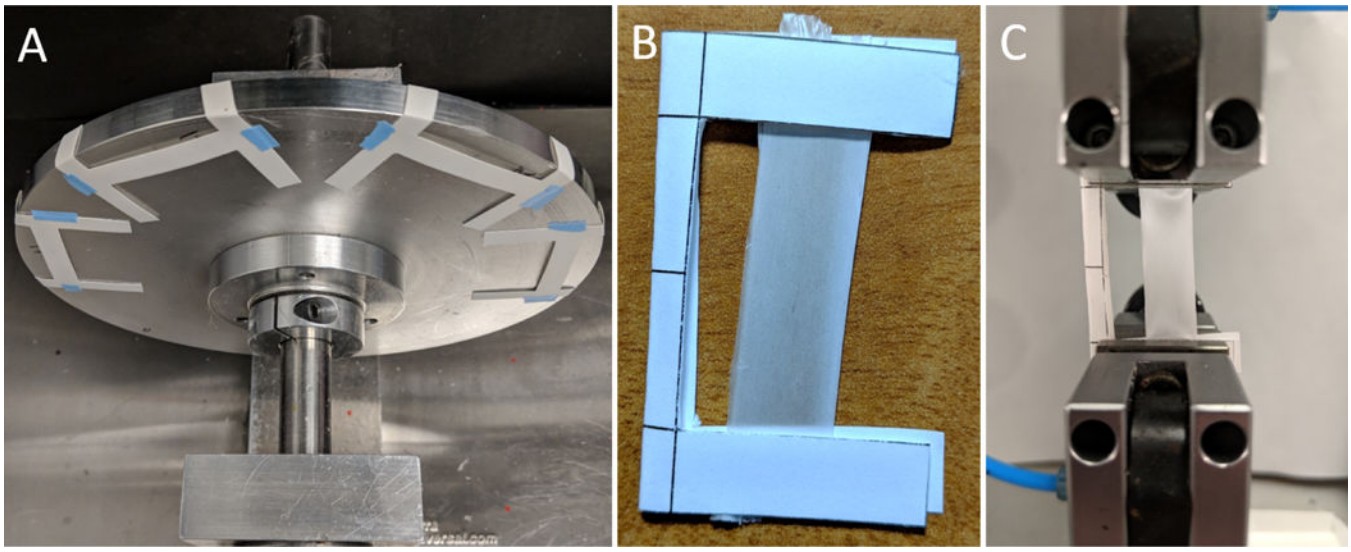

Figure 1.

Electrospinning and tensile testing design for the study. (A) The rotating mandrel used for electrospun fiber collection with mechanical testing I-frames aflxed to the surface onto which fibers collect. (B) An I-frame ready for tensile testing with an electrospun fiber mat secured using double-sided tape. (C) An electrospun fiber mat sample secured in the grips of TestResources universal testing system, prior to tensile characterization.

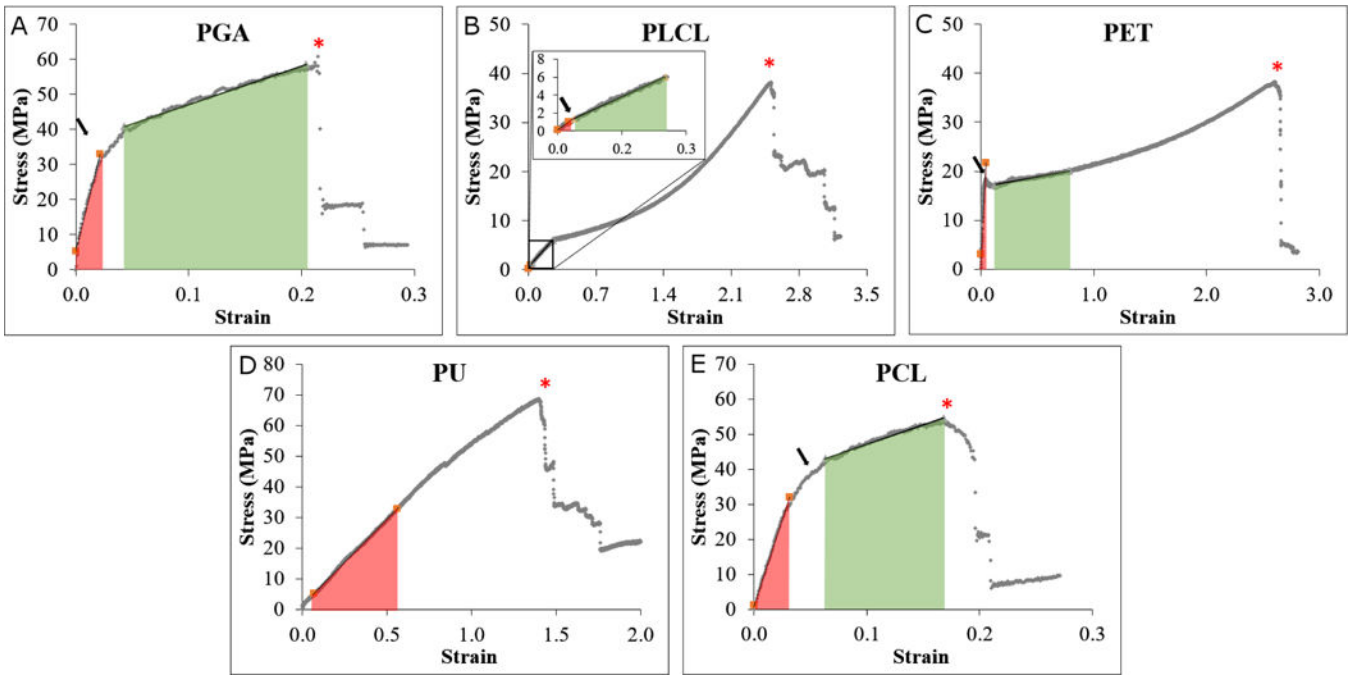

Figure 2.

Representative stress-strain curves obtained via tensile testing of fibers made from (A) PGA, (B) PLCL, (C) PET, (D) PU, and (E) PCL immediately after electrospinning (day 0). PGA, PLCL, PET, and PCL showed bimodal responses to loading and were characterized using elastic modulus (slope in red shaded region), yield strain (black arrows denote yield points), peak stress, failure strain, and failure toughness (red asterisk denotes point of failure). PU showed a linear response to loading with no distinct yield point, and thus had no yield strain.

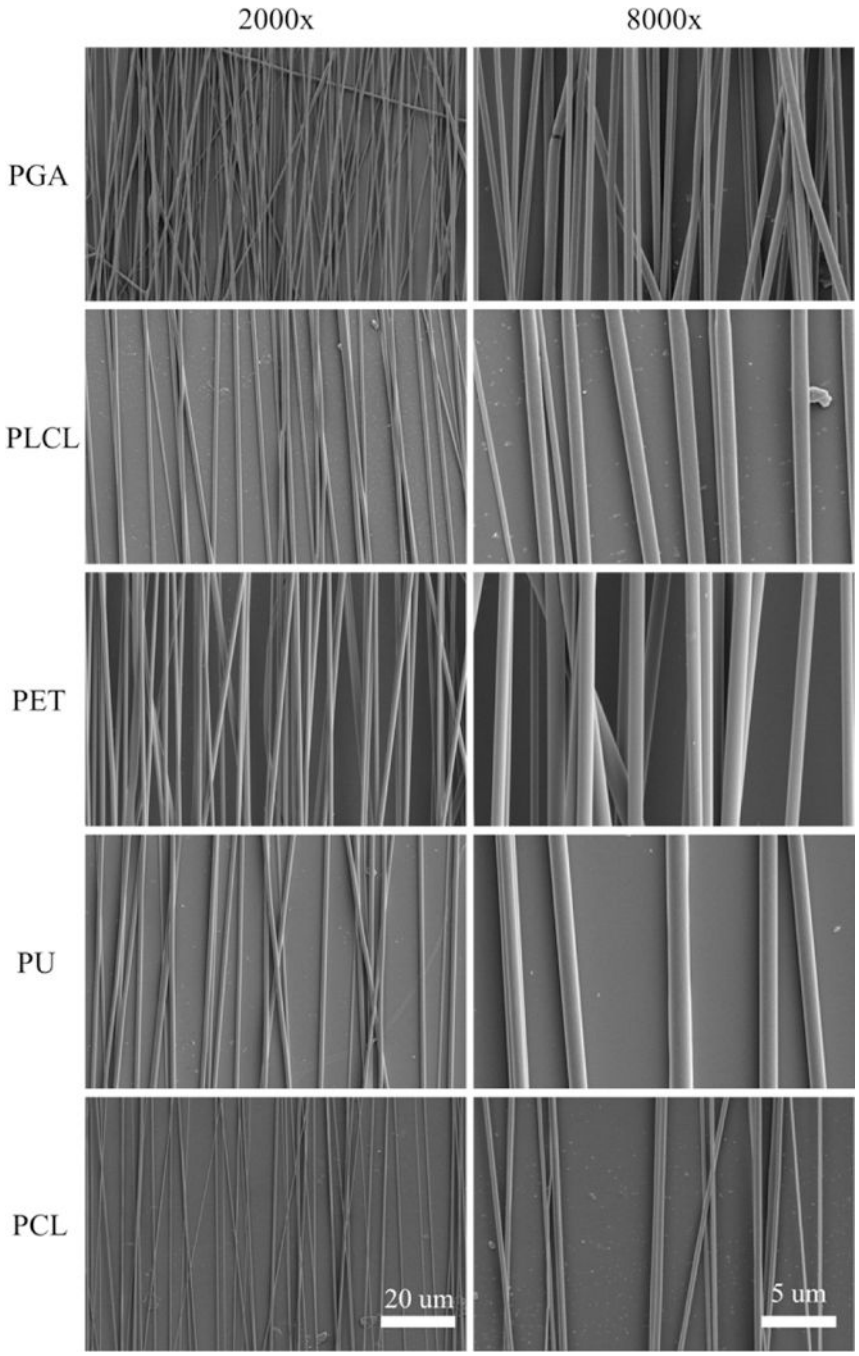

Figure 3.
Scanning electron microscopy (SEM) of electrospun fibers composed of PGA, PLCL, PET, PU, and PCL taken at low (2000x) and high magnification (8000x).

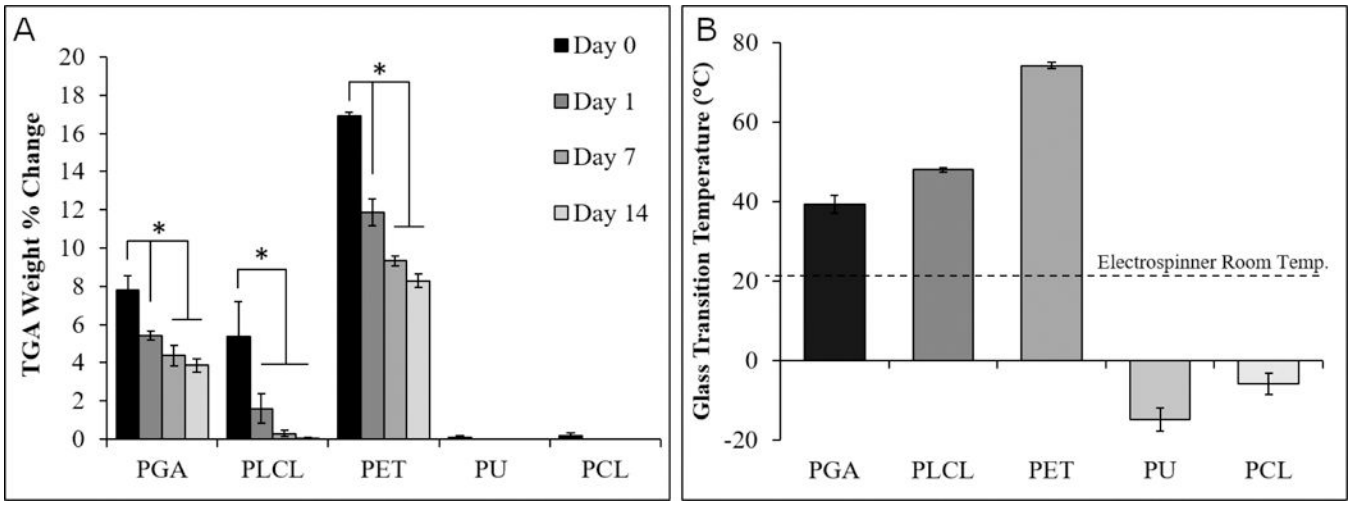

Figure 4.

Electrospun fibers fabricated with different polymers exhibit different solvent retention behavior. (A) TGA results show changes in the weight % of fiber samples that are attributed to solvent retained within the fibers. (B) DSC performed on each type of polymer before any processing was used to determine the T_g values of each polymer type. All data points (represented as bars) from TGA and DSC represent mean values ± standard deviation (N=3). *$p<0.05$ using a one-way ANOVA with post-hoc student's t-test. No statistical analysis was conducted for DSC results since we analyzed T_g values with respect to room temperature rather than differences in T_g between each polymer.

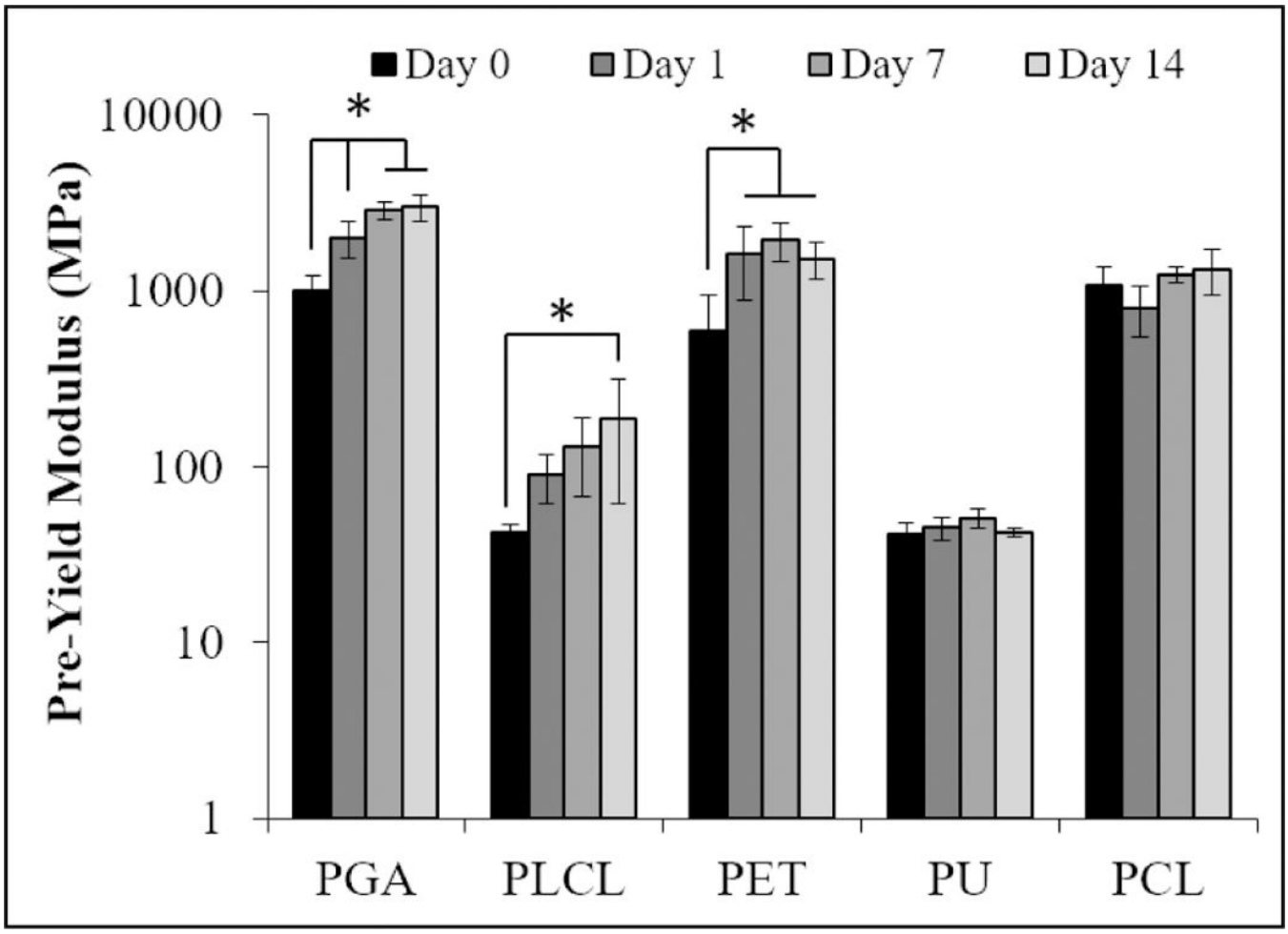

Figure 5.

Characterization of electrospun fiber scaffold elastic modulus. Each bar represents the mean ± standard deviation for three independently fabricated fiber scaffolds. Data are presented on a logarithmic scale. Polymer groups with an * contain time points that are statistically different to other time points within the same polymer. $p<0.05$ using a one-way ANOVA and post-hoc student's t-test.

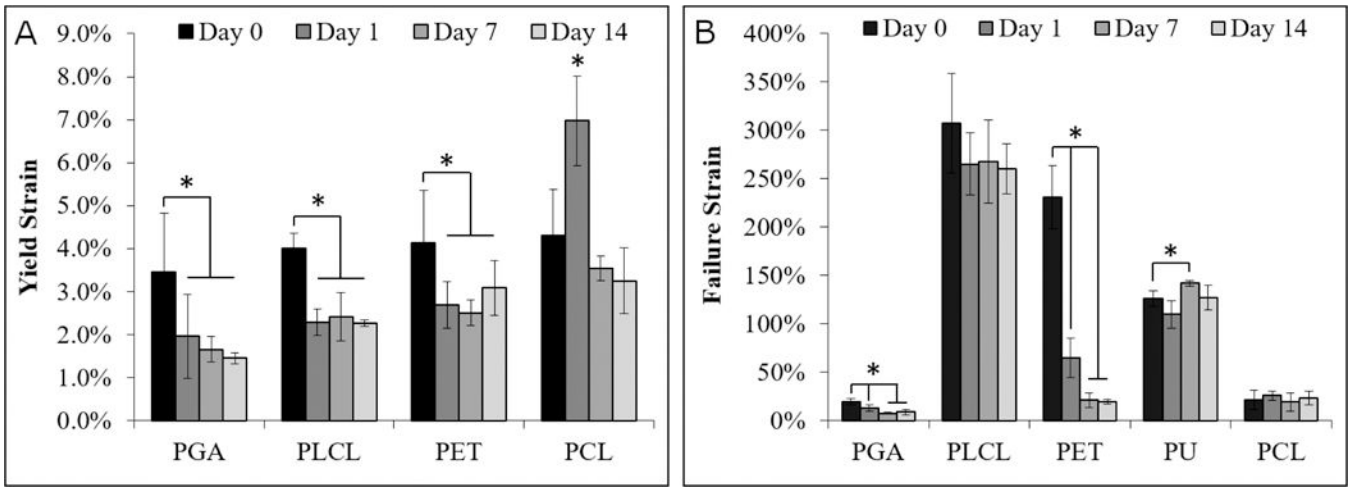

Figure 6.

Characterization of electrospun fiber scaffold (A) yield strain and (B) failure strain. PU is the only polymer of the five that did not exhibit yielding behavior. Each bar represents the mean ± standard deviation for three independently fabricated fiber scaffolds. Polymer groups with an * contain time points that are statistically different to other time points within the same polymer. $p<0.05$ using a one-way ANOVA and post-hoc student's t-test.

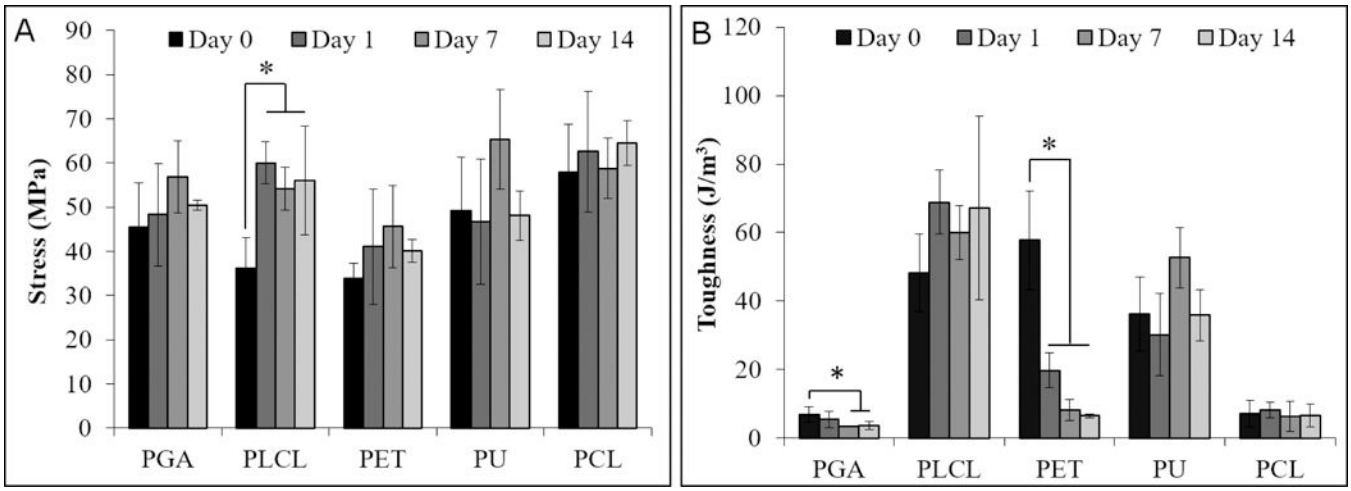

Figure 7.

Characterization of electrospun fiber scaffold (A) peak stress and (B) failure toughness. Each bar represents the mean ± standard deviation for three independently fabricated fiber scaffolds. Polymer groups with an * contain time points that are statistically different to other time points within the same polymer. $p<0.05$ using a one-way ANOVA and post-hoc student's t-test.

Table 1:

Electrospun fiber characterization

Polymer	Fiber Diameter (μm)	Fiber Collection Density (Fibers/mm)	Fiber Coverage (%)	% of Fibers within 15° of mean alignment
PGA	0.48 ± 0.02	1320.0 ± 105.8	64.0 ± 3.8	97
PLCL	1.06 ± 0.04	442.2 ± 27.8	46.9 ± 3.3	100
PET	1.10 ± 0.04	683.1 ± 19.5	75.2 ± 0.9	99
PU	1.16 ± 0.07	244.9 ± 26.8	28.5 ± 4.7	100
PCL	0.36 ± 0.02	544.2 ± 19.5	19.6 ± 0.7	100